RNA Editing Signatures Predict Response to Immunotherapies in Melanoma Patients

Working title: A-I editing and immune response in melanoma.

Jalal Siddiqui[1] and Wayne O. Miles[1*]

1: Department of Cancer Biology and Genetics, Wexner Medical Center, The Ohio State University Comprehensive Cancer Center, The Ohio State University, Columbus, OH.

*: Corresponding author: wayne.miles@osumc.edu

Summary Paragraph

Immunotherapy has improved the prognosis for half of the melanoma patients, prompting a need to understand differences between responding and non-responding patients. Gene expression profiling of tumors has focused on deriving primarily immune-related signatures, however these have shown limited predictive power. Recent studies have highlighted the role of RNA editing in modulating resistance to immunotherapy. This has led us to test whether RNA editing activity can be predictive of response in publicly available datasets of immunotherapy-treated melanoma patients. Here, we identified RNA editing signatures that were able to predict with very high accuracy and confidence patient responses and outcomes. Our analysis, however, demonstrates that RNA editing by itself is sufficient as a strong predictive tool for examining sensitivity of melanoma patients to immunotherapy.

Main

Melanoma is a highly aggressive and frequently lethal cancer. The advent of immunotherapy has significantly improved the prognosis for around half of melanoma patients, however our understanding of which patients will and will not respond to these treatments is a significant hurdle[1-4]. A number of groups have profiled the tumors of melanoma patients on immunotherapy clinical trials utilizing RNA-sequencing (RNA-Seq) in an attempt to identify gene expression signatures associated with patient response[2-4]. Each of these studies have provided important biological insights into genomic and transcriptional changes that drive melanoma, however the predictive power of these signatures is limited.

Recent studies have highlighted the role of RNA editing, particularly by the adenosine deaminase acting on RNA (ADAR) family of proteins as important for the immune response and T-cell activation[5-9]. The ADAR protein family (ADAR1-3 (ADAR3: is

enzymatically inactive)) catalyzes the deamination of Adenines (A) within double-stranded regions of RNA (dsRNA) into Inosines (I), in a process known as A-to-I editing[10]. The resulting I-U base-pair is significantly less stable than the replaced A-U base-pair causing destabilization of dsRNA[10]. These modifications have vital roles in cellular homeostasis, as unedited dsRNA regions are recognized by human cells as viral contaminants and trigger strong immune responses[7,10]. Importantly for our study, the resulting I base is recognized as a Guanine (G) during library construction, enabling the identification of A-I editing sites from RNA-Seq data using a number of available computational tools[11-13]. Based on the strong link between ADAR activity, the immune response and a real need to determine immunotherapy response in patients, we tested the predictive power of RNA editing in publicly available datasets[2,3,11].

Results

Utilizing the Hugo dataset[2], we first examined whether the levels of interferon response or ADAR genes correlated with patient response to immunotherapy. From these results, we found that the expression of interferon (Figure 1a) or ADAR genes (Figure 1b) is not associated with patient outcome (Non-Responder (NR) vs. Responder (R)). In addition, the overall levels of A-I editing events, as measured by AG/TC transitions, also appeared random (Figure 1c, Table S1). We next asked whether RNA editing sites (RES) in independent genes were associated with patient response. For this, we tabulated the RES score[14] for each gene and identified gene RES scores significantly associated with response (t-test $p<0.05$) and not differentially expressed (Wald $p>0.05$)[15,16]. From this analysis, we identified 13 up-regulated (Figure 1d) and 248 down-regulated RES scores (Figure 1e, Table S2) that correlated with patient response to immunotherapy. Down-regulated RES events provided the cleanest clustering of patients based on outcome (Figure 1e). To determine the heterogeneity between patients, we compared the means of the signature RES scores and found a striking and statistically significant difference between non-responding vs responding patients (Figure 1f, Table S3). These findings suggest that RES scores may provide the basis for more accurately predicting patient response to immunotherapy.

Analysis of this type can be affected by confounding factors. To minimize this, we added two additional filtering steps. First, we removed RES scores that had significant linear relationships ($p>0.05$) to transcript levels. Second, we used linear regression on the RES scores with the predictors being response and transcript levels. Following this filtering, we retained only RES scores with a significant response coefficient ($p<0.05$) and removed the confounding effect of transcriptional levels. This approach enabled the identification of 5 up-regulated and 162 down-regulated RES scores that can classify responding vs. non-responding patients (Figures 1g and 1h, Table S2). In agreement with our findings based on the initial criteria, we note that down-regulated RES scores present the most

accurate patient clustering (Figure 1h). The mean RES scores for each of these groups was again tightly correlated with outcome (Figure 1i, Table S3). Importantly, the mean gene expression of these genes was unchanged in responders vs. non-responders (Figure S1a, 1b, Table S3). Collectively, these results show that RES signatures can separate patients by outcome to immunotherapy and that these changes are driven by RNA editing activity and not transcription.

The predictive power of the RES score in the Hugo dataset, compelled us to investigate whether RNA editing signatures could stratify patients from additional cohorts. For this, we selected the Riaz melanoma dataset that included RNA-Seq for melanoma patients treated with nivolumab from the following groups: responder, non-responder, and stable disease patients[3]. In agreement with the Hugo data, an interferon response signature (Figure 2a), ADAR levels (Figure 2b) and gross A-I editing sites (Figure 2c, Table S4), were not predictive. Utilizing our initial RES criteria, we identified gene RES scores that correlated with patient outcome (Figure 2d, 2e, Table S5). This is particularly striking for down-regulated RES sites, as patients that respond to immunotherapy cluster very tightly together (Figure 2e). Mean RES scores across these patient groups also show strong separation in responding patients (Figure 2f, Table S6). Interestingly, patients with stable disease frequently correlate with RES scores of non-responders and show similar RES means (Figure 2d-f). As above, we then filtered these events to remove confounding effects and identified up-regulated (Figure 2g) and down-regulated (Figure 2h) RES scores that tightly correlated with patient outcome. The mean RES scores for each responder is highly significant (Figure 2i, Table S6) and are unchanged at the transcript level (Figure S1c, 1d, Table S6). Collectively, these findings confirm that RES score analysis can be utilized to segregate patients based on their response to immunotherapy. This approach can be used on diverse datasets with differences in sequencing coverage, patient population and immunotherapy agent.

Our RES scores outlined in Figure 1 and 2 correlate with patient response, however we wanted to investigate the predictive power of this pipeline for patients. For this, we used logistic regression models from up and down-regulated mean RES scores from each dataset. Using the Hugo dataset, we found that up-regulated RES scores had a greater than 78% capacity to predict patients that will respond to immunotherapy (Figure 3a, S2a-c, Table S7). We note that the sole responding patient that our model does not predict (blue dot below 0.5 in Figure 3a), is patient 38 (Pt38), which had very high AG/TC levels and is an outlier in Figure 1c. In contrast, the down-regulated RES scores have an over 96% predictive capacity and separates all of the responding patients (Figure 3b, S2d-f, Table S7). In the independent Riaz dataset, we also find that our logistic regression of RES scores predicts patient response with both the up (90%) (Figure 3c, S3a-c) and down-regulated RES genes (Figure 3d, S3d-f, Table S7) having a greater than 87% predictive capacity. Based on these analyses, the down-regulated RES scores represent the most accurate model for determining patient sensitivity. These results highlight the predictive power of this approach for identifying patients that are likely to respond to immunotherapy.

We next evaluated how these RES scores correlated with patient survival. For this, patients were stratified by mean RES scores. For patients with elevated RES scores in the up-regulated group, we find improved survival periods for patients within the Hugo cohort (Figure 3e, Table S8). In agreement, patients with elevated RES score means within the Riaz dataset, show significant survival differences to those with lower means (Figure 3f, Table S8). Although these findings strongly support the predictive power of our model, the down-regulated RES score means show the most significant differences in patient survival (Figure 3g-h, Table S8). In this data, patients with lower mean RES scores display real survival benefit that is independent of the dataset. We next tested how this approach would cluster stable disease patients, and found that this logistic regression test was highly accurate and would cluster these patients with non-responders (Figure S4). Based on the logistic regression model and survival analysis of these patients, the down-regulated RES score enables the most accurate sub-classification of melanoma patients across datasets. This data highlights the predictive nature of RES scores for understanding the clinical benefit for patients on immunotherapy.

We next examined the predictive power of recurrent RES sites within different patient groups. For this, we sub-classified RES sites enriched from responder or non-responder patients. Using recurrent RES sites, we were able to completely separate patients within the Hugo cohort based on clinical response (Figure 4a). This is also true for patients within the Riaz group (Figure 4b), suggesting that recurrent RNA editing within genes is contributing to response. To build on this, we compared the common genes with RES scores within both datasets. These genes with conserved A-I editing were also strongly predictive of patient response and able to segregate responders from non-responders or stable disease in each dataset (Figure 4c, 4d). We then examined whether recurrent RES sites existed between datasets that could predict patient response. For this analysis, we compared RES sites from both datasets and identified 5 RES sites that were present and significant in both (Table S9). We next tested whether these recurrent RES events could separate patients by response, and found that although the number of RES sites is small, these sites correlated with patient response (Figure 4e, 4f). By using the cumulative levels of RES sites within these genes, we find that elevated numbers of RES sites correlate with improved patient survival in both datasets (Figure 4g, 4h). To evaluate the hazard potential of this metric, we utilized Cox Proportional Hazards modeling[17]. From this, we find significant associations between patient response and the number of common RES sites (Table S3, Table S9). Our findings strongly implicate recurrent RES sites within melanoma as predictive of patient outcome and survival.

Discussion

This analysis highlights the real prognostic power of RNA editing sites and the affected genes in predicting immunotherapy responses in melanoma patients. Previous studies have focused on the analysis of genomic and transcriptomic datasets to identify immune

related signatures in pathways such as interferon signaling[18], MHC antigen presentation[3,19,20], and innate anti-PD1 resistance[2]. However, although innovative the predictive power of these signatures to identify patient response to immunotherapy has been limited. In this study, we investigated the capacity of RNA A-I editing events to accurately predict patient outcomes and response to different immunotherapy agents. Our approach has incorporated new knowledge that has been generated by a number of groups that have identified the role of ADAR-mediated RNA editing in development and cancer[5-7,10,21,22]. These studies have linked ADAR activity or ADAR-loss to immune response levels and immune checkpoint blockade. In agreement with a number of other studies, we find no correlation with interferon signatures, ADAR levels or total A-I editing events to immunotherapy response[18,23,24]. However, by systematically identifying A-I RNA changes that do not correlate with transcriptional changes, our RES scores accurately capture A-I editing events that can predict patient response with very high levels of confidence.

These findings show that the RES score is sufficient to predict patient response on vastly different datasets. We note that the significant differences in patient population, library construction and sequencing protocols resulted in more exhaustive coverage in the Hugo dataset compared with Riaz[2,3]. In addition, patients within each trial were treated with different immunotherapies: Patients from the Hugo cohort primarily received pembrolizumab, while the Riaz cohort received nivolumab. In spite of these differences, our data suggests that the controlled use of RNA A-I editing sites is a strong predictive tool for examining the sensitivity of melanoma patients to immunotherapy.

Data Availability

All data are presented in this manuscript are available from the corresponding author upon reasonable request.

Acknowledgements

We would like to acknowledge the support of the Damon Runyon Cancer Research Foundation award 51-18 to W.O.M and the support of a P30 award (CA016058) to the OSUCCC from the National Cancer Institute, Bethesda, MD.

Author Contributions

J.S. conducted the analysis and co-wrote the manuscript. W.O.M conceived the project and co-wrote the manuscript.

Competing Interest

The authors have no competing Interests to declare.

References

1 Wei, S. C., Duffy, C. R. & Allison, J. P. Fundamental mechanisms of immune checkpoint blockade therapy. *Cancer discovery* **8**, 1069-1086 (2018).

2 Hugo, W. *et al.* Genomic and transcriptomic features of response to anti-PD-1 therapy in metastatic melanoma. *Cell* **165**, 35-44 (2016).

3 Riaz, N. *et al.* Tumor and microenvironment evolution during immunotherapy with nivolumab. *Cell* **171**, 934-949. e916 (2017).

4 Van Allen, E. M. *et al.* Genomic correlates of response to CTLA-4 blockade in metastatic melanoma. *Science* **350**, 207-211 (2015).

5 Bhate, A., Sun, T. & Li, J. B. ADAR1: A New Target for Immuno-oncology Therapy. *Molecular cell* **73**, 866-868 (2019).

6 Ishizuka, J. J. *et al.* Loss of ADAR1 in tumours overcomes resistance to immune checkpoint blockade. *Nature* **565**, 43 (2019).

7 Mannion, N. M. *et al.* The RNA-editing enzyme ADAR1 controls innate immune responses to RNA. *Cell reports* **9**, 1482-1494 (2014).

8 Liu, D. *et al.* Integrative molecular and clinical modeling of clinical outcomes to PD1 blockade in patients with metastatic melanoma. *Nature medicine* **25**, 1916-1927 (2019).

9 Auslander, N. *et al.* Robust prediction of response to immune checkpoint blockade therapy in metastatic melanoma. *Nature medicine* **24**, 1545-1549 (2018).

10 Nishikura, K. Functions and regulation of RNA editing by ADAR deaminases. *Annual review of biochemistry* **79**, 321-349 (2010).

11 Zhang, F., Lu, Y., Yan, S., Xing, Q. & Tian, W. SPRINT: an SNP-free toolkit for identifying RNA editing sites. *Bioinformatics* **33**, 3538-3548 (2017).

12 Zhang, Q. in *Transcriptome Data Analysis* 101-108 (Springer, 2018).

13 Picardi, E. & Pesole, G. REDItools: high-throughput RNA editing detection made easy. *Bioinformatics* **29**, 1813-1814 (2013).

14 Chigaev, M. *et al.* Genomic positional dissection of RNA Editomes in tumor and normal samples. *Frontiers in genetics* **10**, 211 (2019).

15 Anders, S. & Huber, W. Differential expression analysis for sequence count data. *Nature Precedings*, 1-1 (2010).

16 Love, M. I., Huber, W. & Anders, S. Moderated estimation of fold change and dispersion for RNA-seq data with DESeq2. *Genome biology* **15**, 550 (2014).

17 Lin, H. & Zelterman, D. (Taylor & Francis, 2002).

18 Alavi, S. *et al.* Interferon signaling is frequently downregulated in melanoma. *Frontiers in immunology* **9**, 1414 (2018).

19 Zhang, M. *et al.* RNA editing derived epitopes function as cancer antigens to elicit immune responses. *Nature communications* **9**, 1-10 (2018).

20 Wang, S., He, Z., Wang, X., Li, H. & Liu, X.-S. Antigen presentation and tumor immunogenicity in cancer immunotherapy response prediction. *Elife* **8**, e49020 (2019).

21 Liu, H. *et al.* Tumor-derived IFN triggers chronic pathway agonism and sensitivity to ADAR loss. *Nature medicine* **25**, 95-102 (2019).

22 Lehmann, K. A. & Bass, B. L. Double-stranded RNA adenosine deaminases ADAR1 and ADAR2 have overlapping specificities. *Biochemistry* **39**, 12875-12884 (2000).

23 Han, J. *et al.* Suppression of adenosine-to-inosine (A-to-I) RNA editome by death associated protein 3 (DAP3) promotes cancer progression. *Science advances* **6**, eaba5136 (2020).

24 Deffit, S. N. & Hundley, H. A. To edit or not to edit: regulation of ADAR editing specificity and efficiency. *Wiley Interdisciplinary Reviews: RNA* **7**, 113-127 (2016).

Methods

Datasets Used

The Hugo dataset (GSE78220) consisted of samples from patients treated primarily with pembrolizumab[1]. 15 were responders and 13 were non-responders based on Immune-related Response Evaluation Criteria In Solid Tumors (irRECIST) criteria[1]. The Riaz dataset (GSE91061) consisted of nivolumab-treated patients of which 23 were non-responders, 10 responders, and 16 stable disease by RECIST criteria[2]. 2 were of unknown response designation[2].

RNA Editing Sites Pipeline

RNA-Seq files were imported from Gene Expression Omnibus (Hugo GSE78220 and Riaz GSE91061) using SRAToolkit 2.9.0. TrimGalore 0.6.0 was used to perform adaptor and quality trimming of RNASeq reads with the additional specification of 6 bases removed from the 5' of each reads[3]. Bowtie2 was used for removing contaminating rRNA and tRNA reads[4]. STAR 2.5.2a was used for aligning the reads to the GRCh38 p12 genome release 31 and obtaining gene counts and BAM alignment files[5,6]. The gene counts were imported into the R environment using *DESeq2*, a Bioconductor package for differential expression analysis and the resulting data was log-regularized[7]. Additionally, a differential expression analysis was conducted between responders and non-responders.

Sprint was used on the resulting BAM alignment files to identify RNA editing sites *de novo*.[8] The *changesammapq.py* script from Sprint was used to convert the BAM files to the correct format for Sprint[8]. The *sprint_from_bam.py* script was used to identify regular RNA editing sites from the resulting BAM file using the GRCh8 p12 genome release 31[6] and Sprint-provided hg38 repeat annotations. Annotating of the resulting RNA editing sites positions for genes, genomic regions, and repeats was done using functions and hg38 annotations from *annotatr*, a Bioconductor package for investigating intersecting genomic annotations[9]. Sprint-provided hg38 repeat annotations were also used in annotating the RNA editing sites.

Identifying Differential RNA Editing

For each gene, we developed an RNA editing score defined as the number of RNA editing sites per gene[10]. For our RNA editing scores, we only focused on A to G or T to C transitions for a gene. The RNA editing scores were log2-transformed with a pseudo-count of 1 to normalize the data. A two-tailed t-test was performed to determine differential RNA editing scores for each gene between responding and non-responding patients with significance criteria being two-tailed p-value < 0.05 and log2 fold change > 0.3785. Additionally, we overlapped the significant genes with DESeq2 results and

removed genes that were differentially expressed at a nominal level of significance (Wald's Test two-tailed p-values < 0.05).

A *final set* of filtering criteria (as opposed to *initial criteria* of filtering by only t-test and *DESeq* results) was developed to remove the influence of log-regularized transcript levels on number of RES identified using linear models analyzed with the *lm()* function in R. Genes with a significant *transcript* two-tailed p-value < 0.05 in *RES ~ transcript* linear model were filtered out. Additionally, the linear model *RES ~ response + transcript* was used to remove transcript levels as a confounding variable and only genes with a two-tailed p-value < 0.05 for the *response* coefficient were retained.

RNA Editing Signatures

The mean RES score of the signature up-regulated and down-regulated gene (for both initial and final criteria) was used as a measure of the RNA editing signatures for each patient sample. Two-tailed pairwise t-tests were conducted between responders, non-responders, and stable disease patients to determine how significantly each signature discriminated between response groups. Additionally, a t-test was also conducted on the corresponding log-regularized transcript levels to determine how the transcript levels of the signature genes significantly discriminated between patient response groups.

Logistic Regression Models

The means of the significant log2-tranformed RNA editing scores from *initial* and *final* up-regulated and down-regulated genes were used as input to a set of logistic regression models using the *glm()* functions in R where *response ~ mean RNA editing score*. Two-tailed p-values of the *mean RNA editing score* coefficient was used to assess significance and model accuracy was calculated for correctly classified patient samples. The *pROC* R package was used for receiver operating characteristic (ROC) analysis[11].

Recurrent RNA Editing Sites

AG/TC RNA editing sites from all samples in each cohort were stratified into sites identified only responders, sites identified only non-responders, and those identified in both responders and non-responders (Stable patients in Riaz were not considered). A two-tailed Fisher's Exact test was performed to determine the contingency of RNA editing sites being enriched in responders or non-responders. Significant recurrent RNA editing sites had a two-tailed p-value < 0.05 and were only annotated to genes with DESeq2 nominal Wald's Test p-values > 0.05. Significant sites whose contingency odds ratio favored responders were responder-enriched and significant sites whose odds ratios favored non-responders were non-responder enriched. For the responder and non-responder enriched RES we determined the annotated genes for these sites using

functions derived from *annotatr*[9]. The responder and non-responder enriched RES and their annotated genes were compared across the Hugo and Riaz cohorts.

Survival Analysis

Survival analyses were done to determine the effects of RNA editing signatures and recurrent RNA editing sites on patient survival. Analyses were performed on all patient samples within a cohort. The *survival* and *survminer* R packages were used[12]. A survival object or response variable was created from survival data using the *Surv()* function. Kaplan-Meir curves were created using the *survfit()* function and Cox proportional hazard regression modeling was done via the *coxph()* function[13]. The *ggsurvplot()* function was used for visualizing survival curves.

References

1 Hugo, W. *et al.* Genomic and transcriptomic features of response to anti-PD-1 therapy in metastatic melanoma. *Cell* **165**, 35-44 (2016).

2 Riaz, N. *et al.* Tumor and microenvironment evolution during immunotherapy with nivolumab. *Cell* **171**, 934-949. e916 (2017).

3 Krueger, F. Trim galore. *A wrapper tool around Cutadapt and FastQC to consistently apply quality and adapter trimming to FastQ files* **516**, 517 (2015).

4 Langmead, B. & Salzberg, S. L. Fast gapped-read alignment with Bowtie 2. *Nature methods* **9**, 357 (2012).

5 Dobin, A. *et al.* STAR: ultrafast universal RNA-seq aligner. *Bioinformatics* **29**, 15-21 (2013).

6 Frankish, A. *et al.* GENCODE reference annotation for the human and mouse genomes. *Nucleic acids research* **47**, D766-D773 (2019).

7 Love, M. I., Huber, W. & Anders, S. Moderated estimation of fold change and dispersion for RNA-seq data with DESeq2. *Genome biology* **15**, 550 (2014).

8 Zhang, F., Lu, Y., Yan, S., Xing, Q. & Tian, W. SPRINT: an SNP-free toolkit for identifying RNA editing sites. *Bioinformatics* **33**, 3538-3548 (2017).

9 Cavalcante, R. G. & Sartor, M. A. Annotatr: genomic regions in context. *Bioinformatics* **33**, 2381-2383 (2017).

10 Chigaev, M. *et al.* Genomic positional dissection of RNA Editomes in tumor and normal samples. *Frontiers in genetics* **10**, 211 (2019).

11 Robin, X. *et al.* pROC: an open-source package for R and S+ to analyze and compare ROC curves. *BMC bioinformatics* **12**, 1-8 (2011).

12 Moore, D. F. *Applied survival analysis using R*. (Springer, 2016).

13 Lin, H. & Zelterman, D. (Taylor & Francis, 2002).

Figure 1: RNA editing sites can segregate melanoma patients based on response to immunotherapy. a) Heat map of Interferon and Interferon-related gene expression changes in non-responder (NR) and responder (R) patients from the Hugo dataset. **b)** ADAR1, ADAR2 and ADAR3 gene expression levels in non-responder and responder patients. **c)** Total AG/TC RNA editing sites vs. total spots in non-responder (red) and responder (blue) patients. **d)** Heat map of up-regulated RES scores in genes using initial criteria in non-responder and responder patients. **e)** Heat map of down-regulated RES scores in genes using initial criteria in non-responder and responder patients. **f)** Means of RES scores of up-regulated and down-regulated genes using initial criteria in non-responder and responder patients. **g)** Heat map of up-regulated RES scores in genes using final criteria in non-responder and responder patients. **h)** Heat map of down-regulated RES scores in genes using final criteria in non-responder and responder patients. **i)** Means of RES scores of up-regulated and down-regulated genes using final criteria in non-responder and responder patients. *p<0.05, **p<0.01, ***p<0.001

Figure 2: RES scores can be used across datasets to sub classify immunotherapy response. a) Heat map of Interferon and Interferon-related gene expression changes in non-responder (NR), responder (R), stable disease (SB) and unknown (UNK) patients from the Riaz dataset. **b)** ADAR1, ADAR2 and ADAR3 gene expression levels in non-responder, stable disease and responder patients. **c)** Total AG/TC RNA editing sites vs. total spots in non-responder (red), responder (blue) and stable disease (orange) patients. **d)** Heat map of up-regulated RES scores in genes using initial criteria in non-responder, responder, stable disease and unknown patients. **e)** Heat map of down-regulated RES scores in genes using initial criteria in non-responder, responder, stable disease and unknown patients. **f)** Means of RES scores of up-regulated and down-regulated genes using initial criteria in non-responder, stable disease and responder patients. **g)** Heat map of up-regulated RES scores in genes using final criteria in non-responder, responder, stable disease and unknown patients. **h)** Heat map of down-regulated RES scores in genes using final criteria in non-responder, responder, stable disease and unknown patients. **i)** Means of RES scores of up-regulated and down-regulated genes using final criteria in non-responder, stable disease and responder patients. *p<0.05, **p<0.01, ***p<0.001

Figure 3: RES scores accurately predict response and survival of melanoma patients to immunotherapy. a) Logistic regression models from the Hugo dataset for up-regulated RES score means and responding prediction for responder (R, blue) and non-responder (NR, red) patients. **b)** Logistic regression models from the Hugo dataset for down-regulated RES score means and responding prediction for responder and non-responder patients. **c)** Logistic regression models from the Riaz dataset for up-regulated RES score means and responding prediction for responder and non-responder patients. **d)** Logistic regression models from the Riaz dataset for down-regulated RES score means and responding prediction for responder and non-responder patients. **e)** Survival analysis of patients stratified by upper 50% (red) and lower 50% (blue) means of up-regulated RES scores for genes in the Hugo cohort. **f)** Survival analysis of patients stratified by upper 50% (red) and lower 50% (blue) means of up-regulated RES scores for genes in the Riaz cohort. **g)** Survival analysis of patients stratified by upper 50% (purple) and

lower 50% (green) means of down-regulated RES scores for genes in the Hugo cohort. **h)** Survival analysis of patients stratified by upper 50% (purple) and lower 50% (green) means of down-regulated RES scores for genes in the Riaz cohort.

Figure 4: Recurrent and common RES sites occur and predict outcomes in melanoma tumors. a) Heat map of significant recurrent RES sites in non-responder (NR) and responder (R) patients from the Hugo dataset. **b)** Heat map of significant recurrent RES sites in non-responder (NR), responder (R), stable disease (SD) and unknown (UNK) patients from the Riaz dataset. **c)** Heat map of significant shared RES genes in non-responder and responder patients from the Hugo dataset. **d)** Heat map of significant shared RES genes in non-responder, responder, stable disease and unknown patients from the Riaz dataset. **e)** Heat map of significant shared RES sites in non-responder and responder patients from the Hugo dataset. **f)** Heat map of significant shared RES sites in responder, non-responder, stable disease and unknown patients from the Riaz dataset. **g)** Survival analysis of patients stratified by common RES number 0-5 from the Hugo dataset (0 common RES - black, 1 common RES – blue, 2 common RES – magenta, 3 common RES – tan, 4 common RES – orange, 5 common RES - red). **h)** Survival analysis of patients stratified by common RES number 0-2 from the Riaz cohort (0 common RES - black, 1 common RES – blue, 2 common RES - magenta).

Figure S1: Gene expression levels of RES containing genes do not correlate with outcome. a) Expression levels of predictive genes that contain up-regulated RES scores in the Hugo dataset. **b)** Expression levels of predictive genes that contain down-regulated RES scores in the Hugo dataset. **c)** Expression levels of predictive genes that contain up-regulated RES scores in the Riaz dataset. **d)** Expression levels of predictive genes that contain down-regulated RES scores in the Riaz dataset. *p<0.05, **p<0.01, ***p<0.001

Figure S2: Logistic models and ROC curves from the Hugo dataset accurately predict patient response. a) Logistic regression models from the Hugo dataset for initial up-regulated RES score means and responding prediction for responder (R, blue) and non-responder (NR, red) patients. **b)** ROC curves of initial up-regulated RES score means. **c)** ROC curves of final up-regulated RES score means. **d)** Logistic regression models from the Hugo dataset for initial down-regulated RES score means and responding prediction for responder (R, blue) and non-responder (NR, red) patients. **e)** ROC curves of initial down-regulated RES score means. **f)** ROC curves of final down-regulated RES score means.

Figure S3: Logistic models and ROC curves from the Riaz dataset accurately predict patient response. a) Logistic regression models from the Riaz dataset for initial up-regulated RES score means and responding prediction for responder (R, blue) and non-responder (NR, red) patients. **b)** ROC curves of initial up-regulated RES score means. **c)** ROC curves of final up-regulated RES score means. **d)** Logistic regression models from the Riaz dataset for initial down-regulated RES score means and responding prediction for responder (R, blue) and non-responder (NR, red) patients. **e)** ROC curves of initial down-regulated RES score means. **f)** ROC curves of final down-regulated RES score means.

Figure S4: Logistic regression models cluster patients with stable disease with non-responders. Graph showing the frequency of stable disease RES scores clustering with non-responders (NR) and responders (R).

a

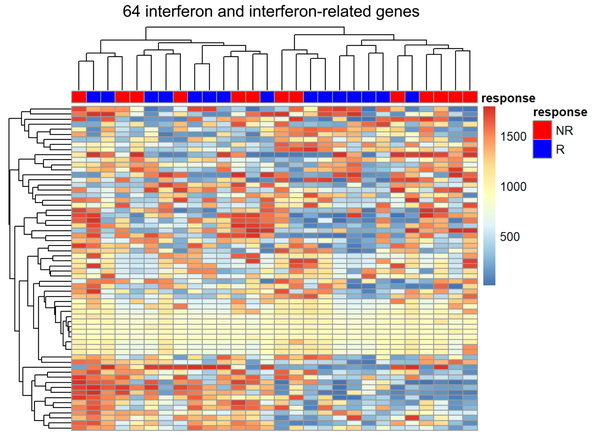

b

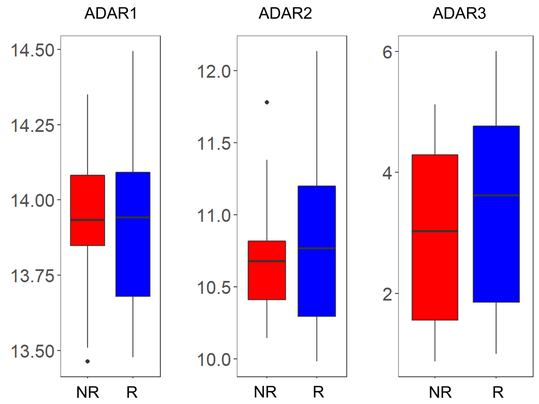

c

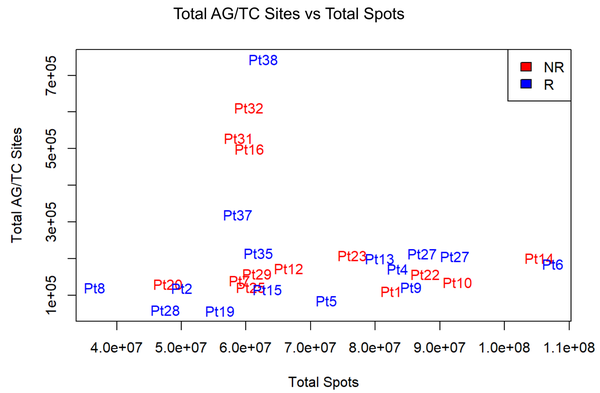

d

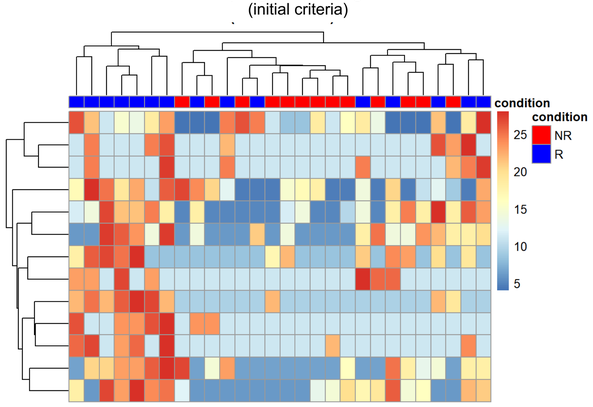

e

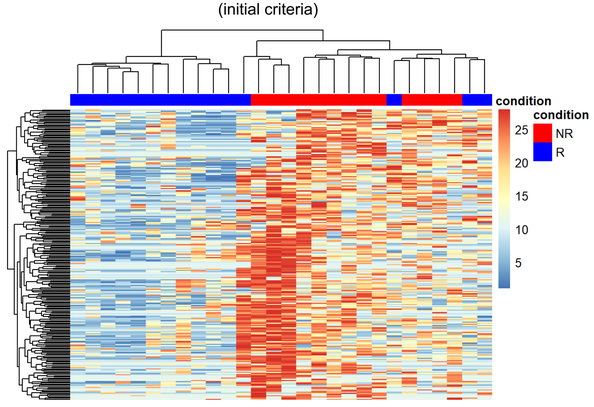

f

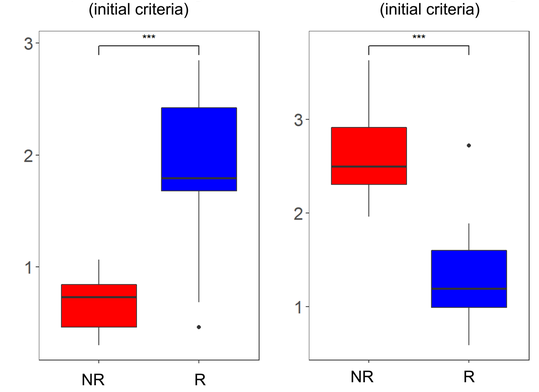

g

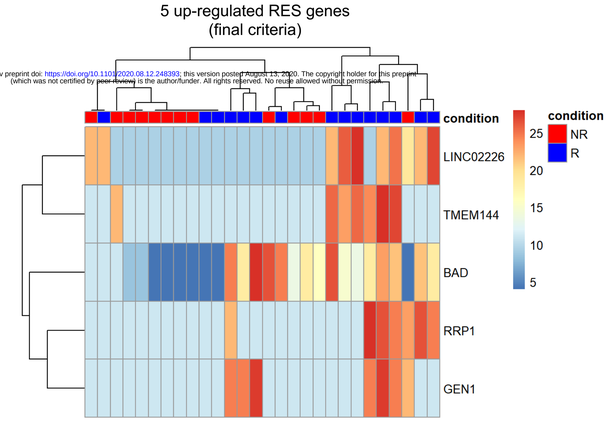

h

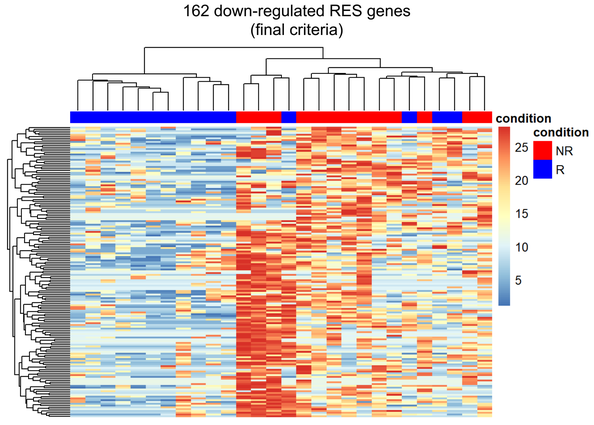

i

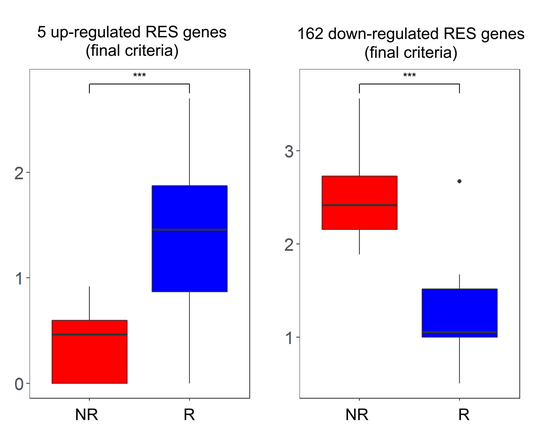

Siddiqui_Figure1

a

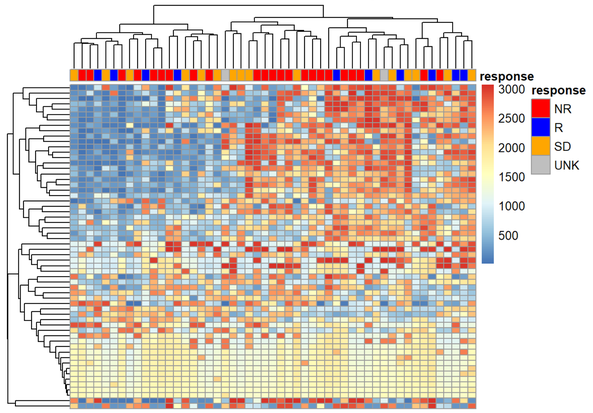

b

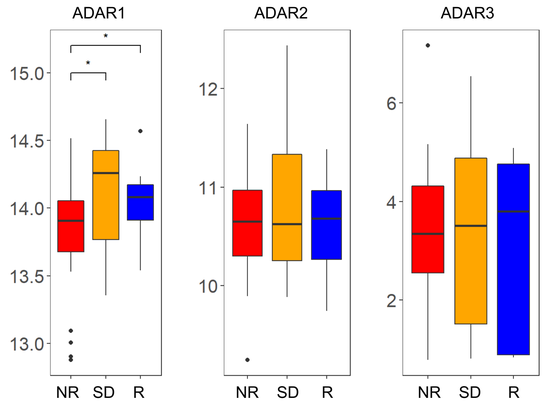

c

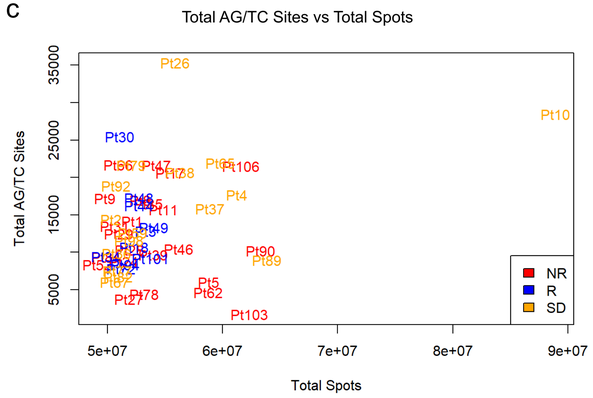

d

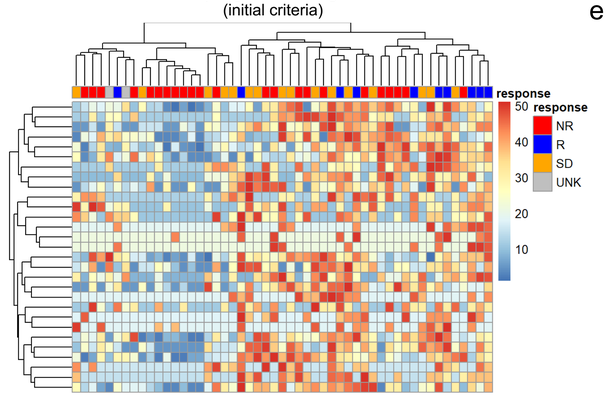

e

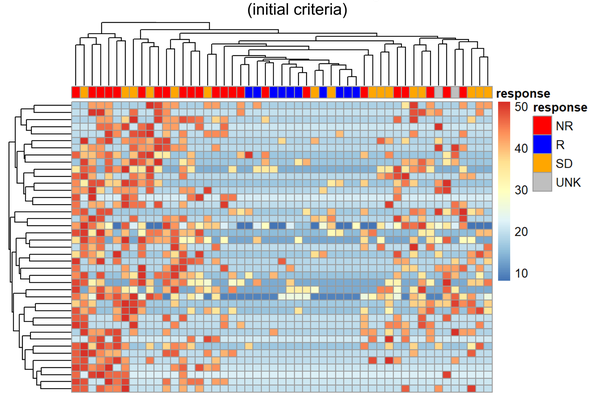

f

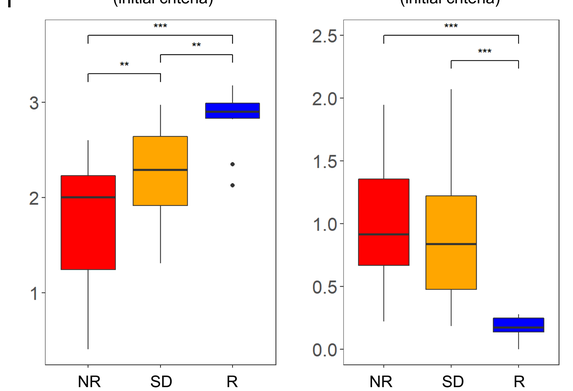

g

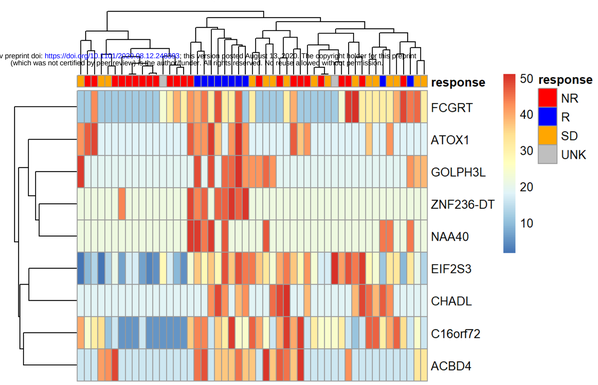

h

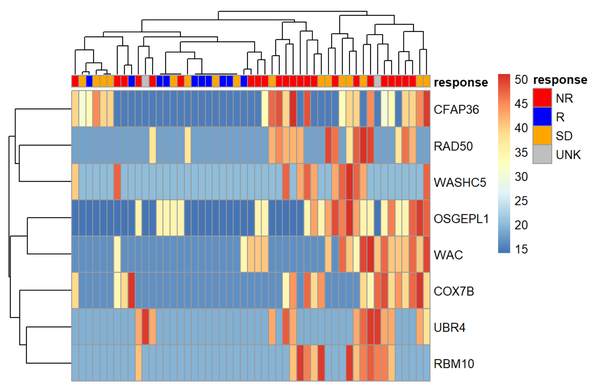

i

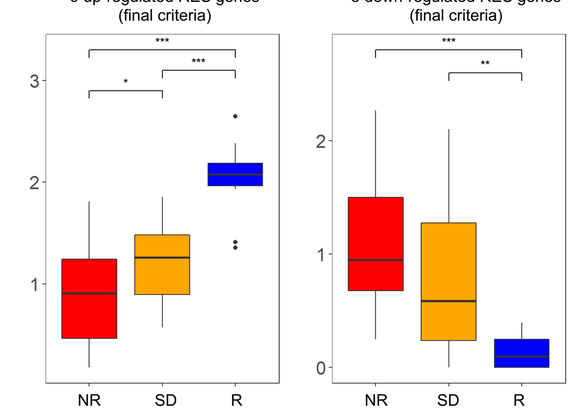

Siddiqui_Figure2

Hugo et al 2016 Cohorts

Riaz et al 2017 Cohorts

a

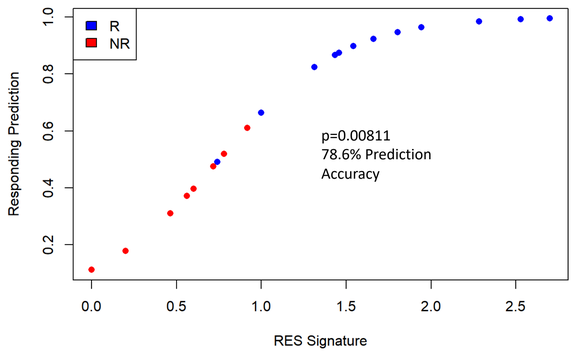

b

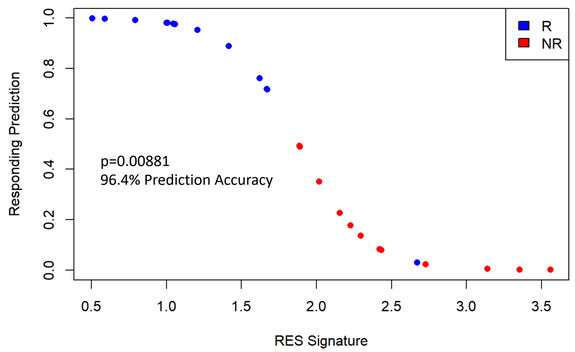

c

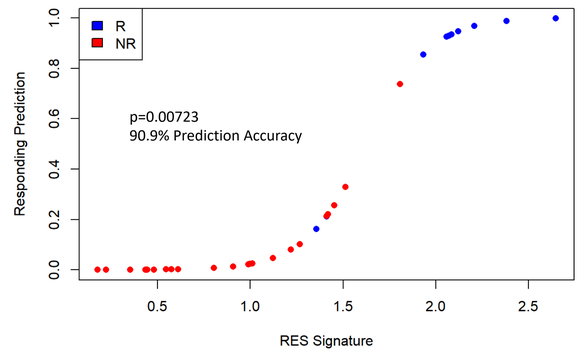

d

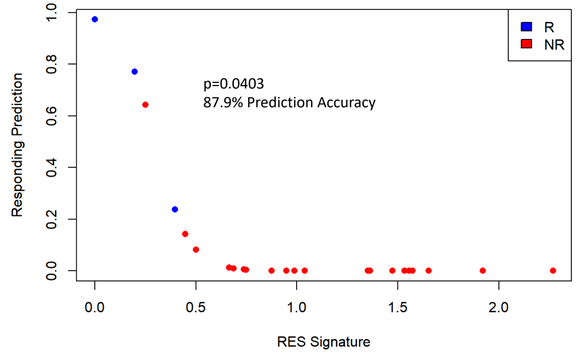

e

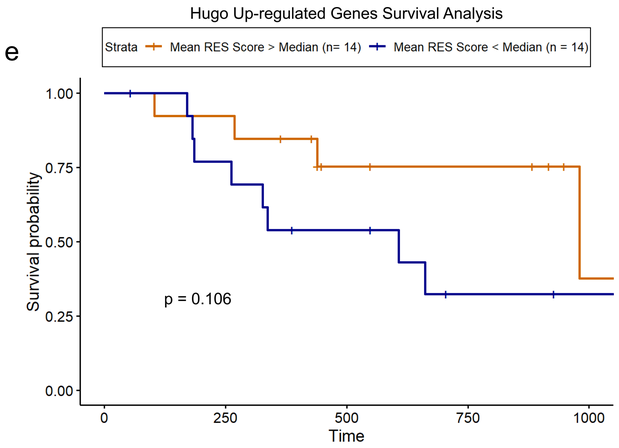

f

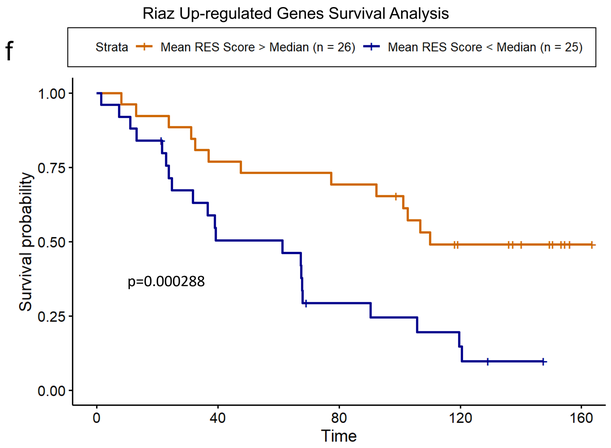

g

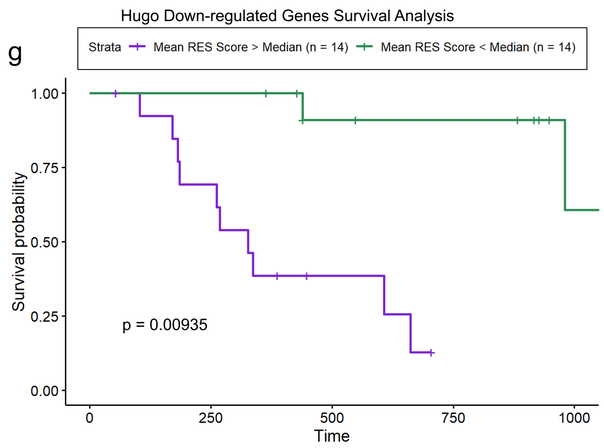

h

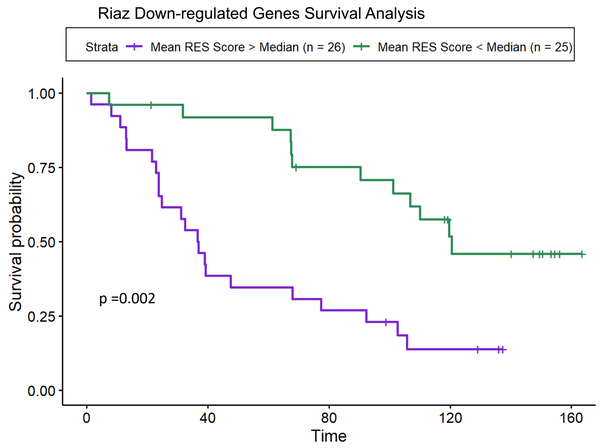

Siddiqui_Figure3

RES from common genes

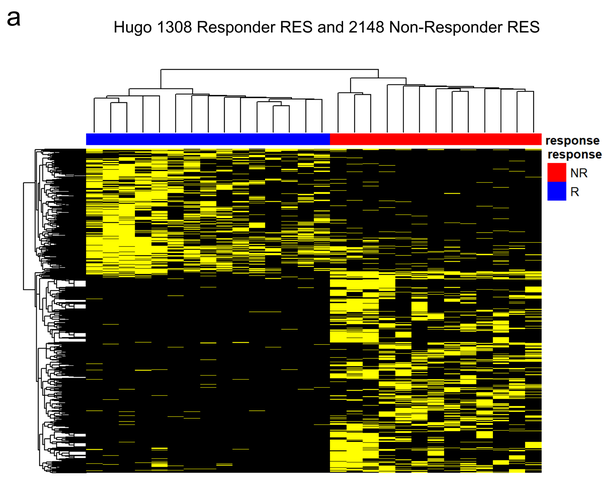

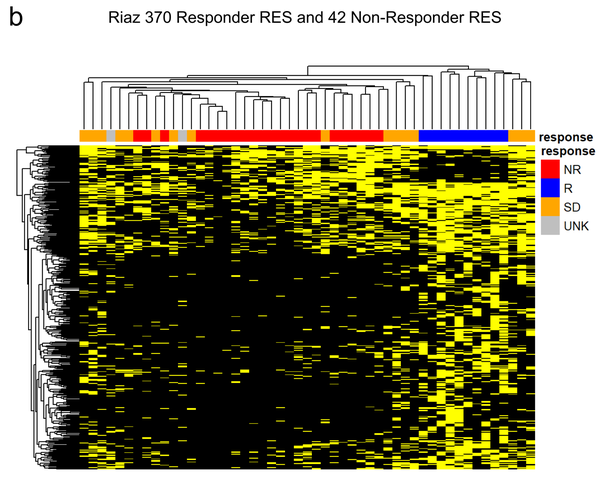

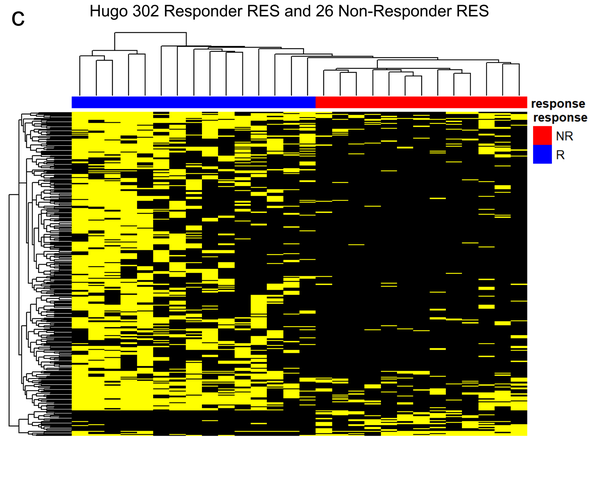

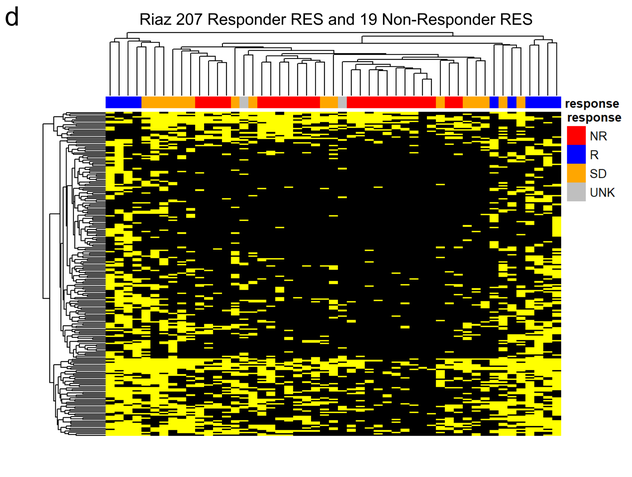

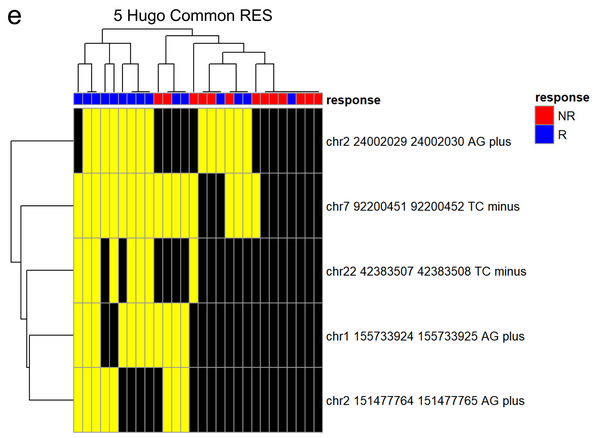

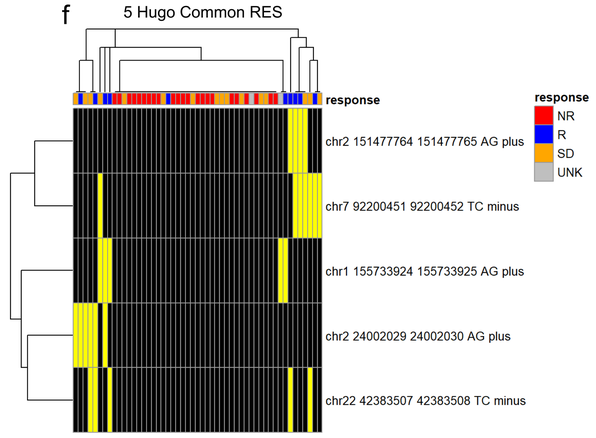

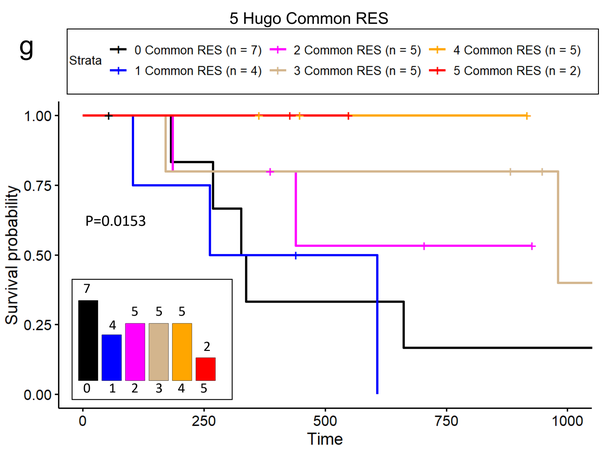

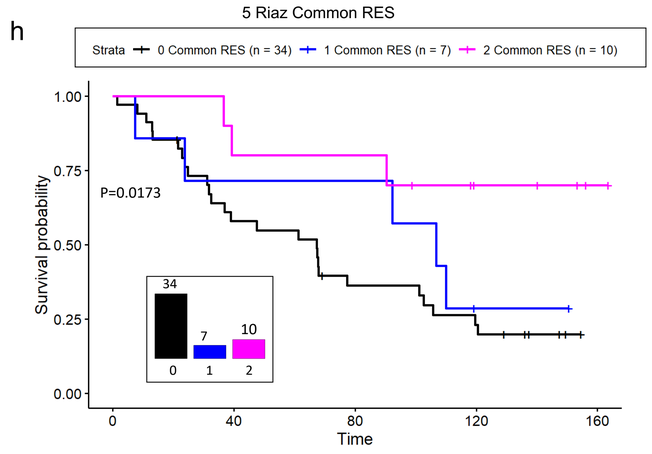

Siddiqui_Figure4

A

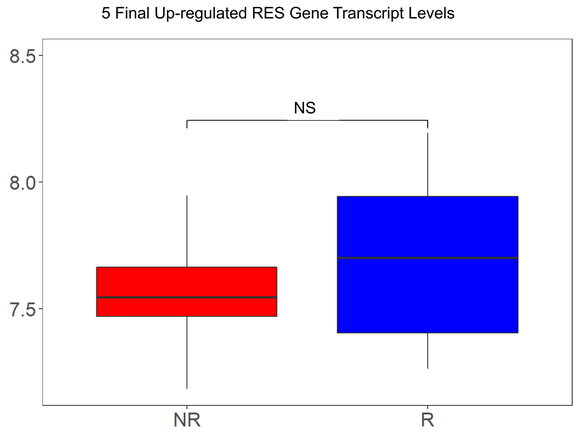

B

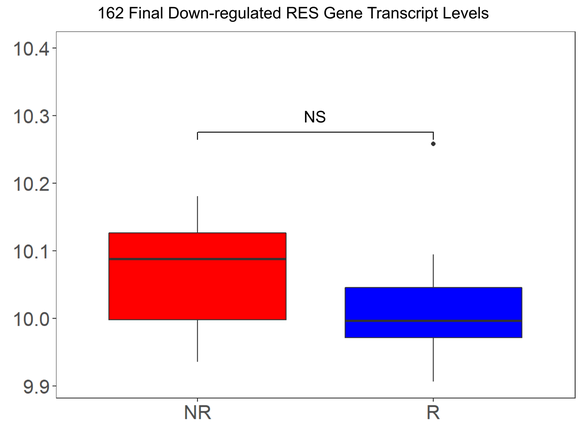

C

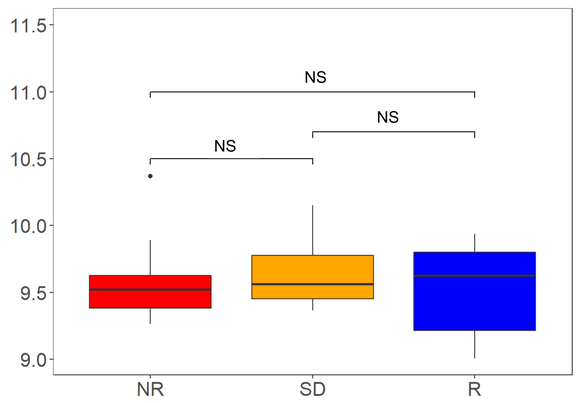

D

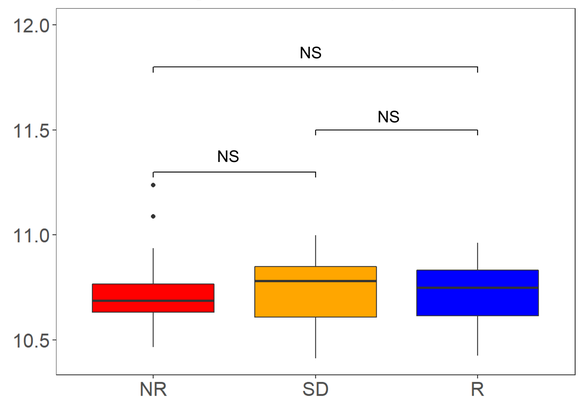

Siddiqui_FigureS1

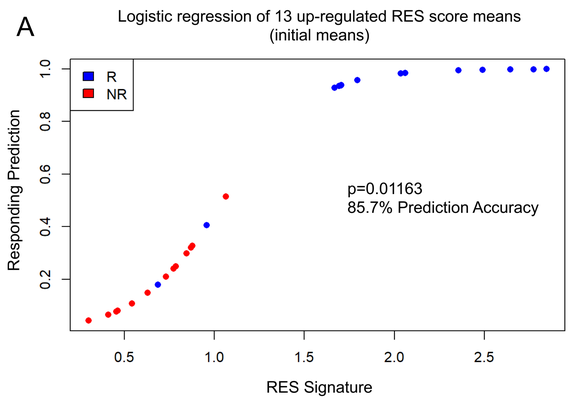

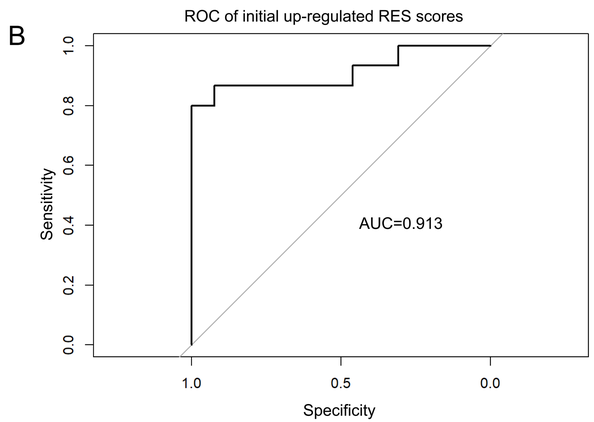

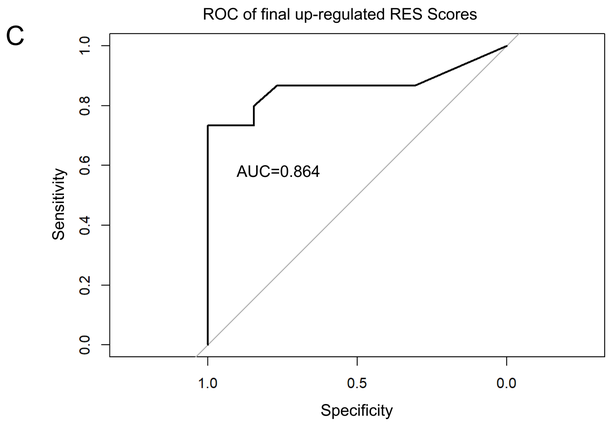

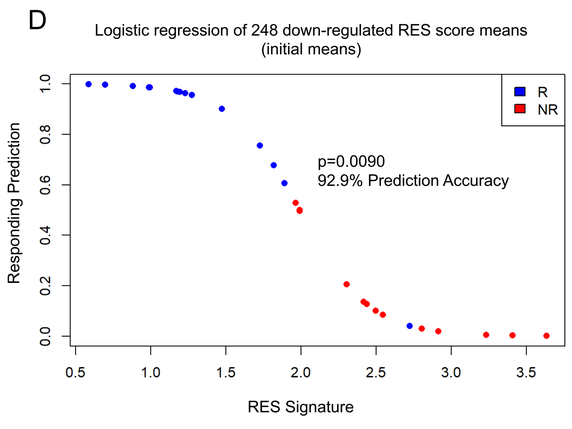

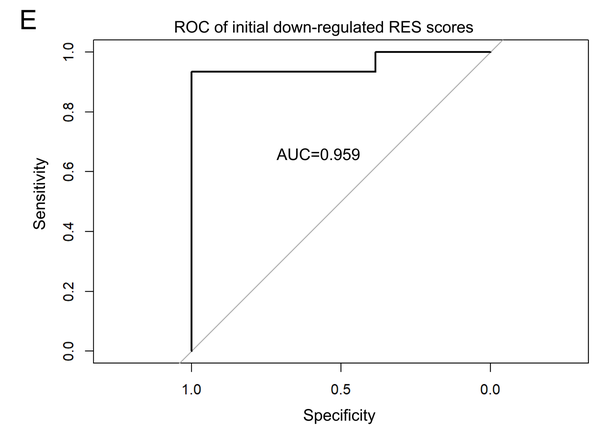

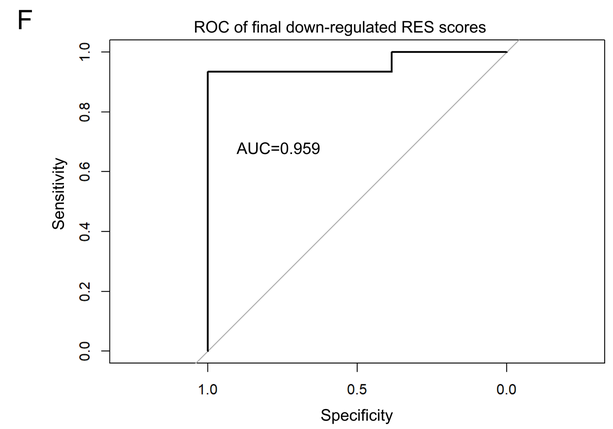

Siddiqui_FigureS2

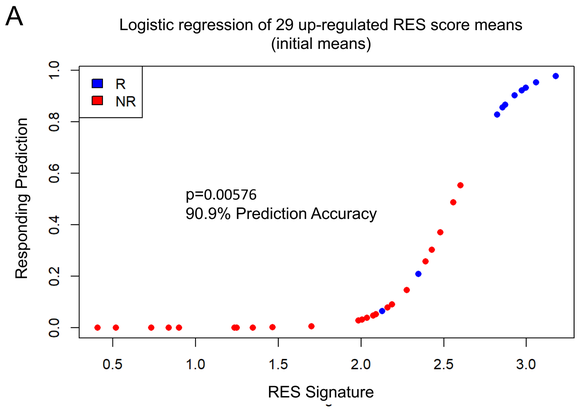

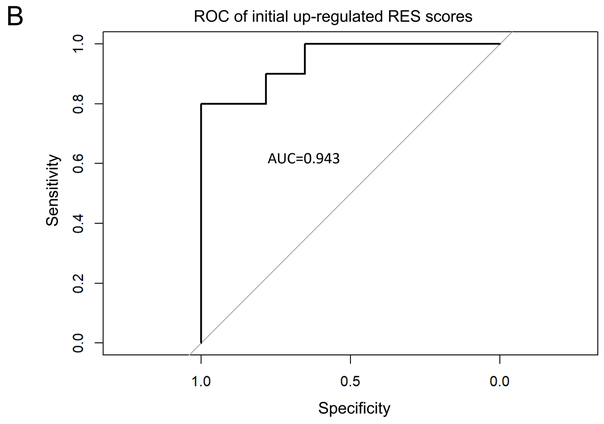

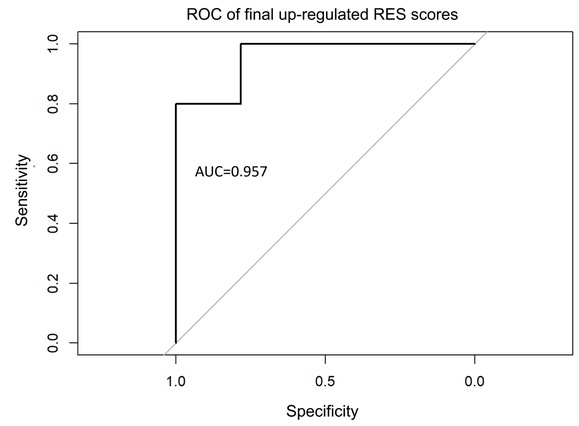

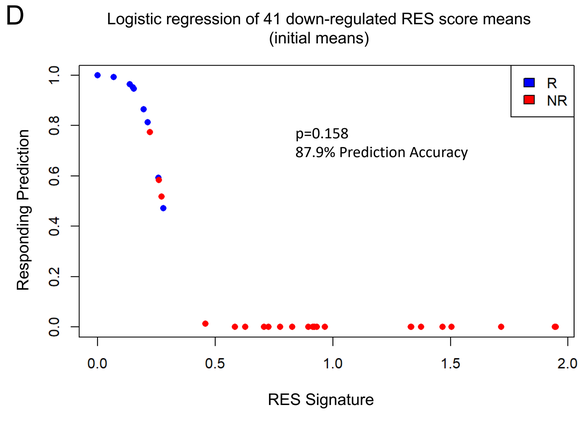

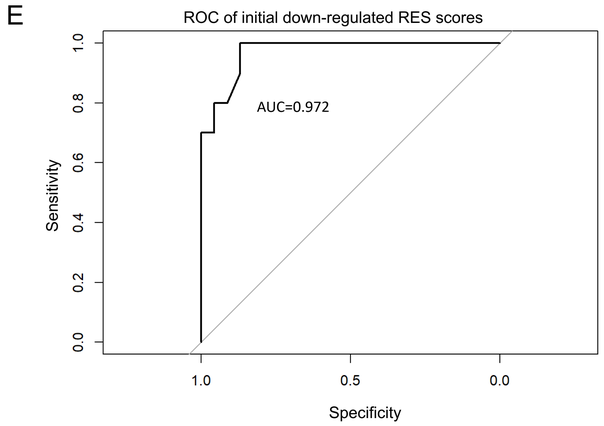

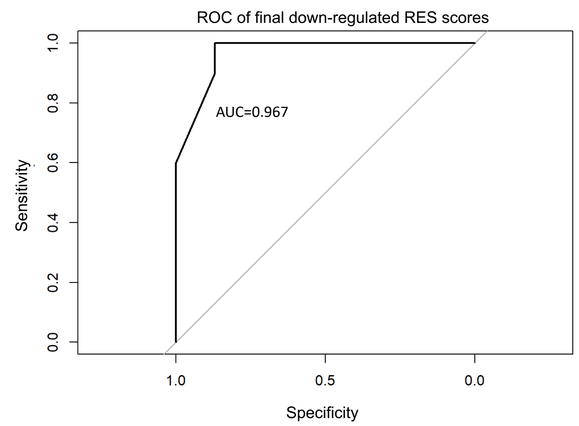

Siddiqui_FigureS3

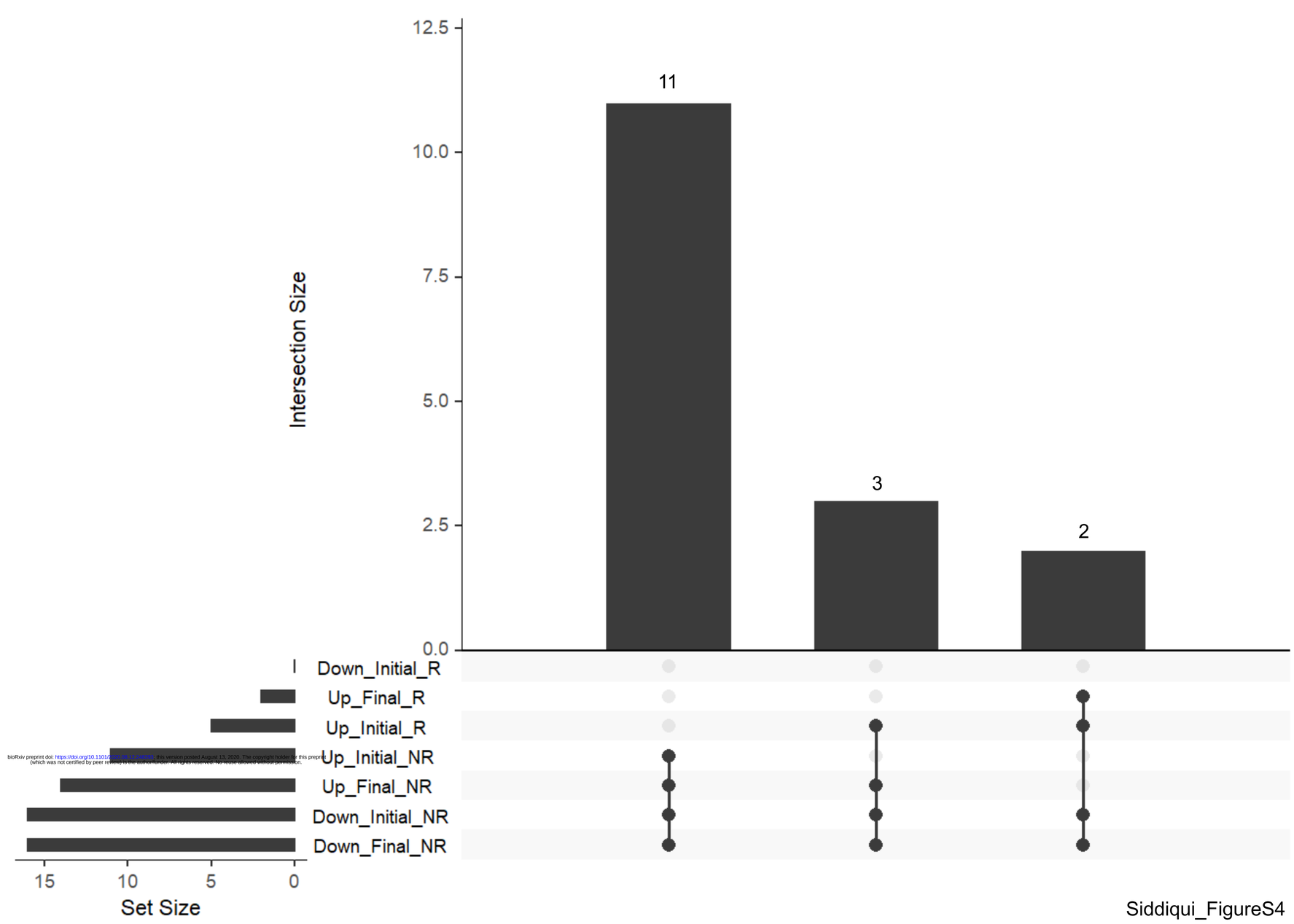

Siddiqui_FigureS4

Table S1: List of Hugo et al, 2016 samples and total RES identified

Sample	Total RES	Total AG/TC RES	Response
SRR3184279	113487	109986	NR
SRR3184280	120503	119098	R
SRR3184281	175009	172171	R
SRR3184282	87648	85321	R
SRR3184283	188339	184670	R
SRR3184284	142434	139986	NR
SRR3184285	122232	120262	R
SRR3184286	125394	120977	R
SRR3184287	139930	135397	NR
SRR3184288	176012	173281	NR
SRR3184289	203427	200152	R
SRR3184290	205424	200691	NR
SRR3184291	119880	115351	R
SRR3184292	514260	499604	NR
SRR3184293	57758	56464	R
SRR3184294	131515	129720	NR
SRR3184295	160197	157045	NR
SRR3184296	212384	207854	NR
SRR3184297	124321	121034	NR
SRR3184298	211518	206137	R
SRR3184299	218569	212844	R
SRR3184300	60642	58878	R
SRR3184301	160617	158044	NR
SRR3184302	552621	528453	NR
SRR3184303	645070	611809	NR
SRR3184304	223249	214872	R
SRR3184305	331579	319552	R
SRR3184306	766700	743066	R

Table S2: RES score signature genes from Hugo et al, 2016 cohort

Initial Up Genes	Initial Down Genes	Final Up Genes	Final Down Genes
BAD	ABHD11	BAD	ABHD11
LINC01184	ACTL6A	LINC02226	ACTL6A
SDCBP2-AS1	ACTR1B	RRP1	ACTR1B
NUDT15	ADAMTSL1	TMEM144	AIDA
SPACA9	AIDA	GEN1	AP3S1
GNGT1	AP3S1		ARG2
LINC02226	ARG2		ASNA1
RRP1	ASNA1		ATN1
ZNF781	ATN1		ATP13A3
FSD2	ATP13A3		ATP8B1
MIR4477A	ATP8B1		BAIAP2L1
TMEM144	AZIN1		BBIP1
GEN1	BAIAP2L1		BCL2L12
	BBIP1		BNIP3L
	BCL2L12		BTK
	BNIP3L		C12orf65
	BRD4		C8orf37-AS1
	BTK		C8orf76
	C12orf65		CBX3
	C17orf67		CCDC142
	C19orf70		CCNB2
	C2orf74		CLN3
	C8orf37-AS1		COQ10B
	C8orf76		CYP51A1
	CALHM2		DARS2
	CAMK1		DCBLD1
	CAVIN1		DDX21
	CBX3		DDX39A
	CCDC136		DEDD
	CCDC142		DNAJC14
	CCNB2		DPM1
	CD109		DRC3
	CERCAM		DSN1
	CGREF1		EAF2
	CLN3		EFCAB13
	COQ10B		EIF3D
	CYP51A1		EMC3
	DARS2		EMC7
	DBF4		ENGASE

	DCBLD1		ERGIC2
	DDX21		ERP44
	DDX39A		EXOC5
	DEDD		FAM200A
	DGKE		FAM210B
	DLGAP1		G3BP1
	DNAJA1		GPN3
	DNAJC14		GSK3A
	DPM1		HMG20B
	DRC3		HMGN2P46
	DSN1		HNRNPU
	EAF2		IPO13
	EFCAB13		IRF3
	EIF3D		KCNJ8
	EMC3		LINC00667
	EMC7		LINC01301
	ENGASE		LOC101927267
	ERGIC2		LPAR6
	ERP44		LSM4
	EXOC5		MAP3K10
	FAAP20		MARCH1
	FALEC		MCEE
	FAM200A		MEAF6
	FAM210B		MEIOC
	FAM92A		MEX3C
	FHL2		NCBP2-AS2
	FKBP10		NECAP2
	FLNB		NIFK-AS1
	FTSJ1		NLRC4
	G3BP1		NOP16
	GBGT1		NRAS
	GCFC2		NUTM2F
	GPN3		PAK4
	GPR153		PCBP2
	GSK3A		PHACTR1
	HMG20B		PMM1
	HMGN2P46		POFUT1
	HNRNPU		PPP2R1B
	HUS1		RALY
	IL17D		RB1CC1
	IPO13		RFK
	IRF3		RNF169
	KCNAB1		ROMO1

	KCNJ8		RUVBL2
	LINC00667		SCCPDH
	LINC01301		SLC38A10
	LOC100130950		SLFNL1-AS1
	LOC101926964		SMIM25
	LOC101927267		SNRPA
	LOC102723729		SNRPD2
	LOC105371049		SNX2
	LOC648987		SPCS2
	LPAR6		SPDYA
	LSM4		SRR
	MAP3K10		STK25
	MARCH1		SUV39H2
	MCEE		TCN2
	MEAF6		TEX10
	MEIOC		TFIP11
	MEX3C		THAP2
	NCBP2-AS2		TRIR
	NECAP2		TUBA1C
	NIFK-AS1		UBE2E2
	NKIRAS1		UBE2J1
	NLRC4		UBL5
	NOP16		WBP2
	NRAS		WDR82
	NUTM2F		YARS
	PAK4		ZBTB11
	PCBP2		ZDHHC4
	PDIA6		ZNF490
	PHACTR1		ZNF827
	PMM1		CPNE5
	POFUT1		EXO5
	POLR3GL		GID8
	PPP1R15B		HEXIM2
	PPP2R1B		PHC1
	PRKDC		PLCB3
	PROSER2		PLTP
	PSIP1		RFC5
	PTER		SLC22A23
	PTGIS		TFAM
	RALY		TUBG1
	RAMP2		AMMECR1L
	RB1CC1		CDC23
	RFK		CENPV

	RNF169		CHAF1A
	ROMO1		EIF2B4
	RUVBL2		HNRNPH1
	SCCPDH		ILF2
	SCNN1D		NFE2L1
	SEC61A1		NPM1
	SLC38A10		ATP2A1
	SLC7A7		GTPBP3
	SLFNL1-AS1		KRT8
	SMIM25		TMED1
	SNRPA		AP2S1
	SNRPD2		NCOR2
	SNX2		RHOBTB2
	SPCS2		SGCB
	SPDYA		SRSF8
	SRR		ADNP2
	SRSF9		CCDC97
	STK17A		CCNB1
	STK25		CDKN3
	SUV39H2		CNTNAP2
	SYTL4		COPS6
	TAF9B		ERO1A
	TCN2		GNAI2
	TEX10		GTF3C5
	TFIP11		MCM2
	THAP2		PKDREJ
	TRIR		SGSM3
	TUBA1C		SYF2
	TUBA8		ZNF81
	TUBB3		RIOK3
	UBE2E2		COX6B1
	UBE2J1		KLHL25
	UBE2L6		SDF2L1
	UBL5		SET
	UGDH		MTFR1L
	WBP2		PLEKHA1
	WDR82		SEMA6A
	YARS		
	YIPF2		
	ZBTB11		
	ZDHHC4		
	ZNF124		
	ZNF490		

	ZNF827			
	CPNE5			
	DEPDC7			
	ENO2			
	EXO5			
	GID8			
	HEXIM2			
	KLHDC2			
	PHC1			
	PLCB3			
	PLTP			
	RFC5			
	RPL18			
	SLC22A23			
	TFAM			
	TUBG1			
	AMMECR1L			
	CDC23			
	CENPV			
	CHAF1A			
	COX6C			
	DACT3-AS1			
	EIF2B4			
	FSCN1			
	HNRNPH1			
	ILF2			
	KDELC2			
	NFE2L1			
	NPM1			
	PGAM1			
	PPP1R26-AS1			
	TIMM44			
	ATP2A1			
	CDC37			
	GTPBP3			
	KRT8			
	TMED1			
	AP2S1			
	CACNB2			
	CDH15			
	FLG-AS1			
	GABRG3			
	MFSD2A			

	NCOR2		
	NPAS1		
	RHOBTB2		
	SGCB		
	SPATA18		
	SRSF8		
	ADNP2		
	C12orf56		
	CCDC97		
	CCNB1		
	CDKN3		
	CNTNAP2		
	COPS6		
	ERO1A		
	EVC2		
	GNAI2		
	GTF3C5		
	HDGFL2		
	LINC01842		
	MCM2		
	PKDREJ		
	SGSM3		
	SLC5A10		
	SYF2		
	TRPV1		
	ZNF81		
	RIOK3		
	CKAP4		
	ZNF597		
	COX6B1		
	KLHL25		
	LMNB2		
	SDF2L1		
	SET		
	MTFR1L		
	PLEKHA1		
	SEMA6A		

Table S3: T-test of Hugo et al 2016 model predictions

Model	Group0	Group1	D.O.F.	Mean Group0	Mean Group1	T-test Statistic	T-test P-value	Diff. of Means
Initial Up RES Scores	NR	R	17.02	0.67	1.86	6.00	1.44E-05	1.19
Initial Down RES Scores	NR	R	25.43	2.63	1.32	-6.33	1.17E-06	-1.30
Final Up RES Scores	NR	R	19.13	0.39	1.41	4.44	2.76E-04	1.02
Final Down RES Scores	NR	R	25.29	2.52	1.22	-6.34	1.18E-06	-1.30
Final Up Transcript Levels	NR	R	25.58	7.56	7.72	1.50	1.46E-01	0.16
Final Down Transcript Levels	NR	R	25.98	10.07	10.02	-1.69	1.02E-01	-0.05

D.O.F. (Degrees of Freedom)

Table S4: List of Riaz et al, 2017 samples and total RES identified

Sample	Total RES	Total AG/TC Sites	Response
SRR5088813	14560	14119	NR
SRR5088887	29306	28448	SD
SRR5088834	9641	9185	R
SRR5088872	1812	1678	NR
SRR5088926	22203	21496	NR
SRR5088916	16108	15677	NR
SRR5088890	21140	20613	NR
SRR5088891	11083	10684	R
SRR5088815	14753	14388	SD
SRR5088818	9335	9032	UNK
SRR5088906	9075	8765	NR
SRR5088920	35971	35303	SD
SRR5088908	3964	3723	NR
SRR5088922	10632	10323	NR
SRR5088909	12812	12475	NR
SRR5088878	13230	12797	R
SRR5088911	25997	25426	R
SRR5088913	13864	13503	NR
SRR5088929	9690	9396	R
SRR5088898	10108	9806	SD
SRR5088900	16295	15830	SD
SRR5088895	21154	20687	SD
SRR5088819	9931	9643	NR
SRR5088880	18138	17665	SD
SRR5088924	16604	16255	R
SRR5088904	10706	10435	NR
SRR5088836	22165	21643	NR
SRR5088897	17623	17268	R
SRR5088824	13629	13326	R
SRR5088883	6286	6023	NR
SRR5088839	8651	8351	NR
SRR5088821	13001	12587	SD
SRR5088856	4934	4644	NR
SRR5088857	22499	21940	SD
SRR5088826	22415	21708	NR
SRR5088840	6187	6025	SD
SRR5088861	8060	7798	R
SRR5088827	13043	12788	UNK
SRR5088846	7804	7475	SD
SRR5088864	4821	4367	NR
SRR5088849	22065	21597	SD

SRR5088914	17364	16941	NR
SRR5088822	7025	6704	SD
SRR5088850	9718	9364	NR
SRR5088829	16919	16451	NR
SRR5088831	9502	8961	SD
SRR5088885	17741	17178	NR
SRR5088866	10496	10181	NR
SRR5088867	19327	18877	SD
SRR5088843	8668	8336	R
SRR5088853	11952	11545	SD

Table S5: RES score signature Genes from Riaz et al, 2017 cohort

Initial Up Genes	Initial Down Genes	Final Up Genes	Final Down Genes
ADGRE2	ACYP1	C16orf72	CFAP36
AUH	ADCY6	EIF2S3	COX7B
C16orf72	C2CD3	ATOX1	RAD50
CTSS	CFAP36	GOLPH3L	UBR4
DTWD2	COX7B	FCGRT	WASHC5
EIF2S3	GIT2	ACBD4	OSGEPL1
FAM129A	GNS	CHADL	WAC
FAM20B	ITCH	ZNF236-DT	RBM10
FPGS	LINC02614	NAA40	
H6PD	MLANA		
KRIT1	MORC3		
LSG1	MYO5A		
PINK1-AS	RAB17		
POLR1E	RAD50		
RALGAPA1	SEC16B		
SOD2	THUMPD3-AS1		
TEP1	TSPAN31		
TRIM56	UBR4		
ATOX1	WASHC5		
FAM111A-DT	ZNF226		
GOLPH3L	ZNF329		
IL12RB1	ZNF426		
LRRC57	ZNF836		
ST3GAL2	GMEB1		
FCGRT	GXYLT2		
ACBD4	OSGEPL1		
CHADL	PRPF3		
ZNF236-DT	SVIL-AS1		
NAA40	WAC		
	ZNF814		
	ZNF718		
	AKAP10		
	FMNL2		
	GOLGA2		
	LOC100130950		
	BICD1		
	ABCA5		
	GON4L		
	GYG2		

	RAF1 RBM10		

Table S6: T-test of Riaz et al 2017 model predictions

Model	Group0	Group1	D.O.F.	Mean Group0	Mean Group1	T-test Statistic	T-test P-value	Mean of Diff.
Initial Up RES Score	NR	R	30.65	1.72	2.82	6.16	8.16E-07	1.09
Initial Up RES Score	NR	SD	36.99	1.72	2.24	2.72	9.84E-03	0.51
Initial Up RES Score	SD	R	23.77	2.24	2.82	3.66	1.26E-03	0.58
Initial Down RES Score	NR	R	25.02	0.99	0.17	-7.42	9.01E-08	-0.81
Initial Down RES Score	NR	SD	30.81	0.99	0.91	-0.47	6.39E-01	-0.08
Initial Down RES Score	SD	R	16.29	0.91	0.17	-5.23	7.73E-05	-0.73
Final Up RES Score	NR	R	20.38	0.87	2.03	7.27	4.38E-07	1.15
Final Up RES Score	NR	SD	35.59	0.87	1.19	2.29	2.84E-02	0.32
Final Up RES Score	SD	R	19.27	1.19	2.03	5.26	4.29E-05	0.83
Final Down RES Score	NR	R	28.00	1.04	0.13	-7.14	8.96E-08	-0.90
Final Down RES Score	NR	SD	26.68	1.04	0.81	-1.05	3.05E-01	-0.23
Final Down RES Score	SD	R	16.95	0.81	0.13	-3.56	2.41E-03	-0.67
Final Up Transcript Levels	NR	R	13.25	9.55	9.52	-0.26	7.96E-01	-0.03
Final Up Transcript Levels	NR	SD	33.87	9.55	9.63	1.00	3.23E-01	0.08
Final Up Transcript Levels	SD	R	14.11	9.63	9.52	-0.89	3.89E-01	-0.11
Final Down Transcript Levels	NR	R	17.63	10.73	10.72	-0.20	8.43E-01	-0.01
Final Down Transcript Levels	NR	SD	32.64	10.73	10.75	0.40	6.89E-01	0.02
Final Down Transcript Levels	SD	R	19.51	10.75	10.72	-0.52	6.09E-01	-0.04

D.O.F. (Degrees of Freedom)

Table S7: Logistic Regression Results

Cohort	Model	Estimate	Standard Error	Z value	P-value	Prediction	ROC AUC
Hugo	Initial Up	4.16	1.65	2.52	0.01	0.86	0.91
Hugo	Initial Down	-4.30	1.65	-2.61	0.01	0.93	0.96
Hugo	Final Up	2.76	1.04	2.65	0.01	0.79	0.86
Hugo	Final Down	-4.46	1.70	-2.62	0.01	0.96	0.96
Riaz	Initial Up	6.10	2.21	2.76	0.01	0.91	0.94
Riaz	Initial Down	-23.66	16.75	-1.41	0.16	0.88	0.97
Riaz	Final Up	5.91	2.20	2.69	0.01	0.91	0.96
Riaz	Final Down	-12.02	5.86	-2.05	0.04	0.88	0.97

Table S8: Cox Proportional Hazards Modeling Results

Cohort	Model	Coefficient	exp(Coefficient)	Standard Error	Z Value	P-value
Hugo	Final Up	-0.63	0.53	0.39	-1.62	1.06E-01
Hugo	Final Down	0.92	2.50	0.35	2.60	9.35E-03
Riaz	Final Up	-1.19	0.30	0.33	-3.63	2.88E-04
Riaz	Final Down	0.75	2.11	0.24	3.09	2.00E-03
Hugo	Common RES	-0.53	0.59	0.22	-2.42	1.53E-02
Riaz	Common RES	-0.63	0.53	0.26	-2.38	1.73E-02

Table S9: Common RES Sites

Chromosome	Start	End	Strand	Transition	Genes
chr1	155733924	155733925	+	AG	DAP3
chr2	151477764	151477765	+	AG	RIF1
chr2	24002029	24002030	+	AG	UBXN2A
chr22	42383507	42383508	-	TC	NFAM1
chr7	92200451	92200452	-	TC	KRIT1